RUNNING HEAD: Discordant genomic and phenotypic clines

TITLE: When polymorphism and monomorphism meet: discordant genomic and phenotypic clines across a lizard contact zone

AUTHORS: Caroline M. Dong[1,2*], Claire A. McLean[1,2], Adam Elliott[1], Adnan Moussalli[2†], Devi Stuart-Fox[1†]

[1]School of BioSciences, The University of Melbourne, Parkville, Vic., Australia

[2]Sciences Department, Museums Victoria, Carlton Gardens, Vic., Australia

*Author for correspondence

†Joint last author

CORRESPONDING AUTHOR

Caroline M. Dong

School of BioSciences, The University of Melbourne, Parkville, Victoria 3010, Australia.

E-mail: caroline.dong@unimelb.edu.au

Abstract

Colour polymorphism can promote rapid evolution and speciation, particularly when populations differ in the number or composition of morphs. The contact zone between *Ctenophorus modestus* (swift dragon) and *C. decresii* (tawny dragon) is a compelling study system in which to examine evolutionary processes and outcomes when polymorphic and monomorphic populations meet. *Ctenophorus modestus* is polymorphic for male throat coloration and lacks ultraviolet (UV) reflectance while *C. decresii* is monomorphic with UV-blue throats. We characterised genomic and phenotypic clines across the contact zone based on single nucleotide polymorphisms, the mitochondrial ND4 gene, and male colour traits, and concurrently assessed the phenotype of captive-bred F1 hybrids. Our results indicate that genomic introgression is asymmetric, with high frequencies of backcrossing to *C. modestus* but not *C. decresii*, accompanied by the prevalence of the *C. modestus* mtDNA haplotype in hybrids. The clines for throat phenotype are abrupt and displaced towards the range of *C. decresii*, relative to the genetic and dorsolateral phenotype clines. By contrast, both throat and dorsolateral phenotypes in captive-bred F1 hybrids are intermediate. Our results are consistent with the hypothesis that throat coloration, a polymorphic sexual signal in *C. modestus*, is the target of selection during incipient speciation and provide insight into the microevolutionary processes that may link polymorphism and speciation.

Keywords: coloration, *Ctenophorus decresii*, *Ctenophorus modestus*, ddRAD, hybridisation, reproductive isolation, speciation

Introduction

Colour polymorphism, the co-existence of multiple colour morphs within a single interbreeding population (Huxley, 1955), is possibly the best studied model of discrete intraspecific phenotypic variation. Recently, there has been great interest in the role of colour polymorphism in promoting rapid phenotypic evolution and speciation, particularly when populations differ in the number, type, and frequency of morphs (Corl, Davis, Kuchta, & Sinervo, 2010; Forsman, Ahnesjö, Caesar, & Karlsson, 2008; Gray & McKinnon, 2007; Hugall & Stuart-Fox, 2012; McLean & Stuart-Fox, 2014; West-Eberhard, 1986). However, we lack detailed studies on the microevolutionary processes linking colour polymorphism and speciation. In particular, the genomic and phenotypic consequences of secondary contact between polymorphic and monomorphic lineages remain unclear, especially where the monomorphic lineage represents a novel morph.

Based on the widespread importance of colour signals in reproductive isolation (Boughman, 2001; Hooper, Griffith, & Price, 2019; Jiggins, Naisbit, Coe, & Mallet, 2001; Mavárez et al., 2006; Sætre et al., 1997; Seehausen et al., 2008) and the predicted genetic architecture of polymorphism (Sinervo & Svensson, 2002), there is expected to be a high probability of incompatibility during secondary contact between populations that differ in morph number, type, or frequency. Gene flow may result in the breakdown of adaptive genetic correlations and generate genetic incompatibilities between morphs (Pryke & Griffith, 2009). More generally, incompatibilities may arise when coadapted alleles are brought together for the first time in hybrids (Dobzhansky-Muller incompatibilities; Dobzhansky, 1937; Muller, 1942) or when coadapted nuclear and organelle (e.g. mitochondria and chloroplast) genomes that evolved in allopatry are disrupted (cytonuclear incompatibilities; Burton and Barreto 2012; Hill 2015). Further, a divergence in sexual phenotypic

65 characteristics may also be accompanied by behavioural incompatibilities in mating
66 preferences resulting in restricted gene flow and/or selection against hybrids. These
67 phenotypic and genetic incompatibilities together may facilitate the process of speciation
68 between populations which differ in morph frequencies and/or composition.

69 Here, we investigate the outcome of contemporary contact between the colour
70 polymorphic *Ctenophorus modestus* (swift dragon; Ahl, 1926) and monomorphic *C. decresii*
71 (tawny dragon; Duméril & Bibron, 1837), previously regarded as divergent lineages of *C.*
72 *decresii* sensu lato (Dong et al., in press). The two species differ in male dorsolateral and
73 throat coloration (Houston 1974; McLean et al. 2014b; Figures 1 and 2a). The polymorphic *C.*
74 *modestus* (previously northern lineage *C. decresii*) has four discrete male throat colour
75 morphs that are present in all populations and reflect little to no ultraviolet (UV): orange,
76 yellow, yellow with orange centre, and grey (Teasdale et al. 2013; Figure 1a). The black
77 dorsolateral stripe of *C. modestus* is relatively straight-edged and continuous, sometimes with
78 one distinct blotch near the neck, and with yellow/orange coloration terminating just behind
79 the shoulder (Figure 2a; McLean, Moussalli, Sass, & Stuart-Fox, 2013). By contrast,
80 monomorphic *C. decresii* (previously southern lineage) males have blue throat coloration with
81 a strong UV reflectance peak, representing a novel morph (Figure 1b; McLean et al. 2014b).
82 Males within an insular population (i.e. Kangaroo Island; "KI") have yellow reticulations in
83 addition to the UV-blue coloration (Figure 2a; McLean et al. 2014b). The black dorsolateral
84 stripe of *C. decresii* is discontinuous with two distinct blotches near the neck and coloration
85 terminating mid-body (Figure 2a; McLean et al., 2013).

86 The throat colour polymorphism is likely to have evolved in *C. decresii* sensu lato and
87 then was subsequently lost in *C. decresii* sensu stricto, thereby facilitating the evolution and
88 fixation of the novel blue morph (McLean, Stuart-Fox, et al., 2014). Genetic divergence

89 between the species (3.7% net sequence divergence in mtDNA) is consistent with range
90 contraction to allopatric refugia during glacial-interglacial Pleistocene cycles (Byrne, 2008;
91 McLean, Stuart-Fox, et al., 2014), where differing site-specific selective pressures may have
92 led to the evolution of divergent phenotypes. A small number of genetically admixed
93 individuals have been identified where the species meet geographically, suggesting that
94 subsequent post-glacial range expansion has resulted in a secondary contact zone (McLean,
95 Stuart-Fox, et al., 2014).

96 This is a compelling study system to explore the evolutionary consequences of
97 hybridisation between colour polymorphic and monomorphic species which differ in morph
98 number and type. Furthermore, the biology of both species and the polymorphism of *C.*
99 *modestus* are well-characterised. *Ctenophorus modestus* and *C. decresii* are sexually
100 dichromatic: females have cream coloured throats with a cryptic dorsal phenotype. Throat and
101 dorsolateral coloration are important intraspecific sexual signals, which are emphasised
102 during complex movement-based territorial and courtship displays (Gibbons, 1977, 1979;
103 Osborne, Umbers, Backwell, & Keogh, 2012; Ramos & Peters, 2016; Stuart-Fox & Johnston,
104 2005). Male throat coloration develops at sexual maturity (ca. 18 months), is fixed for life,
105 and autosomally inherited. The four morphs of *C. modestus* employ alternative behavioural
106 strategies (Yewers, Pryke, & Stuart-Fox, 2016) corresponding to differing hormonal profiles
107 (Yewers, Jessop, & Stuart-Fox, 2017), and are associated with MHC supertypes (Hacking,
108 Stuart-Fox, Godfrey, & Gardner, 2018). The discrete polymorphism is likely controlled by
109 two independently segregating loci, though the extent of orange or yellow within morphs
110 behaves as a quantitative (polygenic) trait (Rankin, McLean, Kemp, & Stuart-Fox, 2016).

111 We used a method of double digest restriction-site associated DNA sequencing to
112 identify single nucleotide polymorphisms (SNPs), sequenced the mitochondrial ND4 gene,

113 and characterised male throat and dorsolateral phenotype across a naturally occurring contact
114 zone between the polymorphic *C. modestus* and monomorphic *C. decresii*. Using geographic
115 cline analysis, we compared the frequency of these genetic and phenotypic traits along a
116 transect through the contact zone from pure *C. modestus* to pure *C. decresii* populations.
117 Furthermore, we conducted captive-breeding to investigate F1 hybrid phenotype independent
118 of exogenous selection. Specifically, we examined i) the geographic extent of hybridisation,
119 ii) whether hybridisation is due to recent or earlier admixture, iii) whether hybridisation is
120 bidirectional or asymmetric, and iv) whether there is evidence of selection on phenotype. We
121 predicted that selection on throat coloration to maintain the *C. modestus* polymorphism
122 should result in steeper and narrower clines compared to SNP and dorsolateral phenotype
123 clines.
124
125 **Materials and Methods**
126 *Field sampling*
127 *Ctenophorus modestus* and *C. decresii* are small [snout-vent-length (SVL) ≤ 90 mm]
128 diurnal rock-dwelling agamids endemic to South Australia. *Ctenophorus modestus* occurs in
129 the Flinders and Olary Ranges whereas *C. decresii* occurs in the Mount Lofty Ranges,
130 Fleurieu Peninsula, and on Kangaroo Island (Figure 2b). The contact zone is found in an area
131 of relatively low-lying grassland between the rocky ranges of the parental species, coinciding
132 with a change from relatively temperate to more semiarid conditions (Houston 1974; McLean
133 et al. 2014b). Our sampling design aimed to capture the full geographic range of both species
134 (Figure 2b, Table S1) to reaffirm previously described genetic divergence based on multi-loci
135 sequence data and microsatellites (McLean, Stuart-Fox, et al., 2014). To extend this previous
136 work we intensively sampled 14 sites along a north-south 160 km transect through the contact

137 zone (Figure 2c, Table S2). As the geographic extent of hybridisation was initially unknown,
138 the transect was anchored on either end by two genetically pure *C. decresii* (southernmost
139 sites 1 – 2) and *C. modestus* (northernmost sites 13 – 14) populations, which were
140 geographically connected along a rock range. Sites were demarcated by geographic distance
141 when possible; however, areas with high densities of sampling were demarcated more finely
142 to allow greater accuracy in analyses. Lizards were captured with a lasso (telescopic pole and
143 fishing line) or by hand and released at the site of capture following data collection. A genetic
144 sample (blood or tail tip stored in 99% ethanol at -20°C) and phenotypic data (described
145 below and in Supplementary Information) were taken from each individual. We focused on
146 collecting data from adult males (SVL ≥ 65 mm) and collected genetic samples from females
147 opportunistically. Our dataset comprised 234 genetic samples in total from across both
148 species' full ranges (Table S1, Figure 2b). This included 152 genetic samples from the 14
149 sites along the contact zone transect, from which we also obtained phenotypic data from up to
150 233 males along the contact zone transect, depending on the trait (Table S2).

151 *SNP discovery*

152 Genomic DNA was isolated and purified from blood or tissue using either an E.Z.N.A.
153 Tissue DNA Kit (Omega Bio-tek, Norcross, GA, USA) or a GenCatch Blood and Tissue
154 Genomic Mini-Prep Kit (Epoch Life Sciences, Sugar Land, TX, USA). DNA was sent to
155 Diversity Arrays Technology (Bruce, ACT, Australia) for SNP genotyping using DArTSeq, a
156 genome complexity reduction method similar to double digest restriction-site associated DNA
157 (ddRAD) sequencing protocol. Protocols are described in detail for broad applications in
158 Kilian et al., 2012 and specifically for the genus *Ctenophorus* in Melville et al., 2017. Briefly,
159 genomic DNA was digested with two restriction endonucleases (PstI/HpaII), PCR amplified
160 (1 min at 94°C; 30 cycles of 94°C for 20 s, 58°C for 30 s, 72°C for 45 s; final extension at

161 72°C for 7 min), and sequenced on an Illumina HiSeq2500. 'High-density' DArTseq SNP
162 arrays use 2,500,000 (±7%) reads per sample in marker calling. Two technical replicates of
163 each DNA sample were genotyped to assess reproducibility. DArT analysis pipelines and a
164 calling algorithm (DArTsoft14) were used to process sequences into a matrix of SNP loci. As
165 reference genomes, we used the *C. decresii* sensu lato draft genome (McLean, Stuart-Fox, and
166 Moussalli, unpublished data) and the fully annotated central bearded dragon genome (*Pogona*
167 *vitticeps;* Georges et al., 2015). In total, we obtained 172,893 SNPs from 234 individuals with
168 41.54% missing data. Using the R package *dartR* (v1.1.6, Gruber et al. 2018), we filtered this
169 dataset conservatively with thresholds of 100% reproducibility, ≤1% missing data per locus,
170 ≤10% missing data per individual, and also removed loci that deviated from Hardy-Weinberg
171 Equilibrium ($P < 0.05$). This resulted in a dataset of 1,333 SNPs from 230 individuals with
172 0.26% missing data. Additionally, to evaluate potential bias associated with stringent filtering,
173 we repeated the filtering steps with a threshold of ≤5% missing data per locus (other
174 thresholds unchanged), resulting in a dataset of 6,889 SNPs from 225 individuals with 1.46%
175 missing data. Analyses run on this dataset indicated qualitatively similar results (Figure S1).
176 *Mitochondrial DNA*
177 We sequenced an 850 base-pair region of the mitochondrial genome which included
178 the NADH dehydrogenase subunit four (ND4), and tRNAhis, tRNAser and tRNAleu regions
179 using the primers ND4F (Forstner, Davis, & Arèvalo, 1995) and tRNA-Leu (Scott & Keogh,
180 2000) for a subset of 74 individuals from sites across the contact zone transect (Table S1).
181 PCR was performed following procedures in McLean, Stuart-Fox, et al., 2014. PCR products
182 were submitted to the Australian Genome Research Facility (Melbourne, Victoria, AUS) for
183 purification and forward and reverse sequencing on an Applied Biosystems 3730xl DNA
184 Analyzer. Sequences were edited and aligned with additional ND4 sequences spanning the

185 range of *C. modestus* and *C. decresii* (McLean, Stuart-Fox, et al., 2014) in Geneious (v6.1.7;
186 Kearse et al. 2012). Haplotype networks were constructed using the statistical parsimony
187 algorithms of TCS (v1.21; Clement et al. 2000).

188 *Quantifying population structure and admixture*

189 We examined genome-wide patterns of divergence using the Bayesian model-based
190 clustering approach implemented in STRUCTURE (v2.3.4; Pritchard, Stephens, & Donnelly,
191 2000). After an initial burn-in of 500,000 Markov chain Monte Carlo (MCMC) generations,
192 we ran 500,000 generations with 10 independent replicates for K values ranging from 1 to 5
193 under the "admixture" model with correlated allele frequencies and prior population
194 information, all other parameters were kept at default, and convergence of runs was visually
195 assessed. We used STRUCTURE HARVESTER (Earl & VonHoldt, 2012) to identify the
196 optimum value of K for our dataset and summarised results across the selected value of K
197 using CLUMPP (v1.1.2; Jakobsson & Rosenberg, 2007). We used the Bayesian estimation of
198 the *q*-value (proportion of an individual's genome inherited from each parental population)
199 with 95% confidence intervals (CI) as a hybrid index. Individuals were identified as pure
200 parentals or putative hybrids based on their hybrid index and 95% CI: an individual was
201 classified as parentals if *q* was less than 0.1 (i.e. *C. modestus*) or greater than 0.9 (i.e. *C.*
202 *decresii*), or of mixed ancestry if *q* was between 0.1 and 0.9.

203 We used previously identified population groups within each parental lineage to
204 further examine population structure (*C. modestus*: Northern Flinders Ranges [NFR],
205 Southern Flinders Ranges [SFR], Olary Ranges [OR]; *C. decresii*: Mainland South [MS],
206 Kangaroo Island [KI]; McLean et al. 2014b) and Contact Zone (CZ). We calculated expected
207 and observed heterozygosity, the number of alleles and allelic richness, estimated population
208 pairwise F_{ST}, and the inbreeding coefficient (F) for each population using the R packages

209 *dartR* (v1.1.6; Gruber et al. 2018) and *adegenet* (v2.1.1; Jombart & Ahmed, 2011). We then
210 performed a principal coordinate analysis (PCoA) using *dartR* to visualize pairwise genetic
211 distances between individuals.

212 *Hybrid classification*

213 We subsampled our SNP dataset to obtain a dataset of 200 loci with the highest
214 average polymorphic information content values using the R package *dartR* (v1.1.6; Gruber et
215 al. 2018). The dataset was analysed three times in parallel, each with a total of 100,000
216 MCMC generations after an initial burn-in of 50,000 generations, using the program
217 NewHybrids (v1.1 Anderson & Thompson, 2002) and the R package *parallelnewhybrid*
218 (Wringe, Stanley, Jeffery, Anderson, & Bradbury, 2017). We determined the probability that
219 individuals within the contact zone belonged to one of the six genotypic classes resulting from
220 the first two generations of hybridisation: parental forms (P1 and P2), F1 (P1 × P2), F2 (F1 ×
221 F1), and backcrossed (F1 × P1/P2). Although it is not always possible to unambiguously
222 assign individuals into discrete classes due to the continuum that may be found in wild
223 populations, classification may be suggestive of situations where contact is very recent or
224 where F1 hybrids are infertile based on the absence of F2 hybrids and backcrosses, or where
225 contact is several generations old based on the absence of pure parentals and F1 hybrids.

226 *Inferring population history*

227 We estimated population demographics with the program δaδi v2.0.6 (Gutenkunst,
228 Hernandez, Williamson, & Bustamante, 2009, 2010), which uses a diffusion approximation
229 method to analyse joint site frequency spectra. For this analysis we considered only
230 geographically connected populations of *C. modestus* and *C. decresii*, and therefore excluded
231 NFR and KI from the dataset (Figure 2). The full set of SNPs (i.e. 172,893 SNPs from 234
232 individuals) was filtered with a threshold of ≤5% missing data per locus, ≤10% missing data

233 per individual and 100% reproducibility, and secondaries were removed (i.e. retained one
234 SNP per locus) to reduce linkage disequilibrium (filtering performed in *dartR* (v1.1.6, Gruber
235 et al. 2018). This resulted in a dataset of 4,956 SNPs from 212 individuals with 1.48%
236 missing data, which we converted to δaδi input format using the R package *radiator* (v1.1.5;
237 Gosselin, Lamothe, Devloo-Delva, & Grewe, 2020).

238 We implemented a modified version of the model optimisation workflow
239 (dadi_pipeline) from Portik et al., 2017. We were specifically interested in inferring the age of
240 the contact zone and therefore tested two biologically realistic models of population history
241 consistent with the observed structure of the contact zone: 1) "sec_contact_asym_mig", where
242 the two species split with no migration (T1), followed by a period of asymmetrical migration
243 (T2; Figure 4); and 2) "sec_contact_asym_mig_three_epoch", a more complex model
244 involving a period of isolation after secondary contact (T3; Figure S2). Both models
245 considered two geographically structured 'populations', on either side of the density trough
246 between sites 2 and 3 (Figure 2): 1) *C. decresii* (MS; Figure 2) and 2) *C. modestus* pooled
247 with admixed individuals (OR, SFR and CZ; Figure 2). We used folded site frequency
248 spectra, a grid size of 200, 220, 240 and projection sizes of 60 and 180 alleles for *C. decresii*
249 and *C. modestus* respectively. For each model, we performed two independent runs with four
250 consecutive rounds of optimisation, with 100 replicates per round, increasing maximum
251 iterations (maxiter = 5, 5, 10, 20), and decreasing fold in parameter generation (fold = 3, 2, 2,
252 1). Models were compared using the log-likelihood and Akaike information criterion (AIC),
253 and the two independent runs converged on similar parameters (Table S5). We converted
254 parameters from the top model as follows: reference effective population size as $N_{ref} = \frac{\theta}{4\mu l}$,
255 where θ was the scaled population parameter, μ was a mutation rate of 9×10^{-10} (Singhal &
256 Moritz, 2013) and l was the length of analysed sequence (4956 SNPs × 70b = 34.7Mb);

257 population size as $Nu = N_{ref} \times nu$; time as $T = t2N_{ref} \times g$ where g was a generation time

258 of 2 years; and migration (individuals per generation) as $M_{ij} = \left(\frac{m_{ij}}{2 \times Nref}\right) \times nu_i$.

259 *Captive-breeding and testosterone-induced expression of colour traits*

260 To evaluate F1 hybrid phenotype independent of extrinsic selection pressures, we

261 conducted captive breeding using 36 pure *C. decresii* individuals (female = 17, male = 19)

262 collected from cline site 1 (southernmost site, longitude: 139.103°, latitude: -33.443°) and 41

263 pure *C. modestus* individuals (female = 20, male = 21) from cline site 14 (northernmost site,

264 longitude: 139.103°, latitude: -33.443°; Table S2, Figure 2c) to produce reciprocal cross

265 hybrids, in addition to pure offspring for comparison. Offspring were housed individually and

266 reared under laboratory conditions (total = 138; southern = 11, northern = 54, hybrids = 73).

267 We genotyped adults and offspring at five microsatellite loci (Am41, Cp10, Ctde45, Ctde05,

268 Ctde12; Schwartz et al. 2007; McLean et al. 2014b) and confirmed paternity using a

269 maximum likelihood approach in CERVUS (v3.0.7; Kalinowski, Taper, & Marshall, 2007;

270 Marshall, Slate, Kruuk, & Pemberton, 1998). For all offspring, we induced throat colour

271 expression by artificially elevating testosterone levels at nine months of age in both sexes

272 (female = 64, male = 74; supplemental information). Females can be reliably induced to

273 express discrete throat morphs found in males using testosterone because throat coloration is

274 autosomally inherited; testosterone may influence the intensity of coloration but morphs

275 remain objectively classifiable (Rankin & Stuart-Fox, 2015). Dorsolateral colour patterns

276 remained unchanged in testosterone-treated females therefore dorsolateral phenotype was

277 analysed only for male offspring. See Supplemental Information for full details of breeding,

278 rearing, genotyping, and throat colour expression procedures.

279 *Analysis of phenotypic data*

280 To characterise the phenotype of wild-caught males and captive-bred F1 hybrids, we
281 took standardised ventral (i.e. throat) and dorsal photographs and spectral reflectance
282 measurements of throat colours (details in Supplementary Information). The standardised
283 photos were used to classify throats into existing morphs (orange, yellow, orange-yellow,
284 grey, or blue), and to quantify the proportion of orange and yellow coloration present on the
285 head and neck from dorsal photographs. We also manually quantified the number of distinct
286 breaks in the dorsolateral stripe near the neck by visually inspecting all photographs of the
287 dorsal region. Spectral reflectance measurements (300 – 700 nm) were used to estimate the
288 receptor quantum catch (QC), the stimulation of retinal photoreceptors, for the violet to UV
289 wavelength sensitive (UVS) photoreceptor because we were specifically interested in the
290 diagnostic UV-blue component of throat coloration.
291 We performed principal component analyses (PCA) to explore variation in throat
292 coloration variables (proportion of orange, proportion of yellow, proportion of blue) and
293 dorsolateral phenotype variables (proportion orange, proportion of yellow, breaks in the
294 dorsolateral stripe) in the R package *FactoMineR* (v1.4.1; Le, Josse, & Husson, 2008). In
295 each, the lineages were differentiated along the first dimension (PC1) and this was used to
296 collapse variables into a single measure of overall phenotype and retained for use in
297 subsequent cline analyses. The quantum catch of the UV sensitive photoreceptor (QC_{UVS}) was
298 used singly in cline analyses to assess its frequency across the contact zone independent of
299 throat colour morph. Due to missing data, 204 individuals were used in throat phenotype
300 analyses whereas 233 individuals were used in dorsolateral phenotype analyses. Linear
301 discriminant analyses were performed on pure individuals in the R package *MASS* (v7.3.50;
302 Ripley, 2002) using all throat phenotype variables (proportion of orange, yellow, and blue,
303 and QC_{UVS}) and dorsolateral phenotype variables as independent variables.

304 *Geographic cline analysis*

305 We used the R package *HZAR* (v0.2-5, Derryberry, Derryberry, Maley, & Brumfield,
306 2014) to fit a series of equilibrium geographic cline models (Gay, Crochet, Bell, &
307 Lenormand, 2008; Szymura & Barton, 1986; Szymura & Barton, 1991) to both the molecular
308 and phenotypic datasets, and in all cases using 1,000,000 MCMC generations following an
309 initial burn-in of 100,000 generations. Specifically, we estimated cline models for the hybrid
310 index (H_{Index}; Bayesian *q*-value based on 1,333 loci), mtDNA haplotype frequencies, quantum
311 catch of the UV wavelength sensitive receptor (QC_{UVS}), PC1 for throat coloration (T_{PC1}), and
312 PC1 for dorsolateral phenotype (D_{PC1}).

313 *HZAR* uses logistic regression equations to fit sigmoidal clines in a maximum-
314 likelihood framework and describes cline centre (*c*) as the position where estimated trait
315 frequency is 0.5 and width (*w*) as 1/slope at the cline centre. For molecular clines, we
316 compared 15 models that varied in the fitting of trait interval (*p*; minimum and maximum
317 frequencies at tails; fixed at 0 and 1, observed values, estimated values) and exponential
318 decay tails (none, right only, left only, mirrored, both estimated separately). These 15 models
319 were compared to an additional null model. For phenotypic trait data we compared models
320 that varied in the fitting of exponential decay tails (none, right only, left only, mirrored, both
321 estimated separately) and estimated mean and variance on the ends and in the centre. All
322 models estimated cline centre and width as well as tail parameters if applicable (δ, distance
323 from the centre to the tail; τ, tail slope). QC_{UVS} and T_{PC1} were normalised to values between 0
324 and 1 for plotting purposes.

325 To address model selection uncertainty, we conducted model averaging in an Akaike's
326 information criterion (AIC) framework. We calculated the Akaike weight (AIC*w*), a value
327 between 0 and 1 which can be interpreted as the probability of being the best approximating

328 model (Burnham & Anderson, 2002). Models were then ranked by AIC*w* downwards until the
329 cumulative AIC*w* reached 0.95 to attain a 95% confidence set of best-ranked models (Lukacs,
330 Burnham, & Anderson, 2010; Symonds & Moussalli, 2011). We recalculated the AIC*w* of
331 models in the 95% confidence set and used those to calculate the model-averaged estimate of
332 parameters (e.g. centre and width). We produced model-averaged clines by first multiplying
333 the estimate for a given distance interval by the AIC*w*. This was done for each model within
334 the 95% confident set of models. The AIC model averaged estimate was then obtained by
335 summing up weighted estimates for each distance interval. Similarly, we multiplied the
336 minimum and maximum estimate bounds by the AIC*w*, followed by summation to represent
337 the credible region. Finally, the coincidence of cline centres was assessed by comparing
338 model-averaged maximum-likelihood derived CIs (two log-likelihood unit support limits) of
339 cline centres, with non-overlapping CIs considered statistically supported differences. Akaike
340 weights were calculated using the R package *MuMIn* (v1.43.6; Bartoń 2018).
341
342 **Results**
343 *Population structure and admixture*
344 We found distinct population genetic structure within *C. modestus* and *C. decresii*, and
345 evidence for the presence of hybrids in the contact zone. Based on the STRUCTURE analysis,
346 only two clusters were identified, corresponding to the major split between *C. modestus* and
347 *C. decresii* (Figure 2d, Table S3). The *q*-values ranged from 0.999 (pure southern) to 0.001
348 (pure northern). Across the contact zone transect, individuals from the southernmost sites 1 –
349 2 had a high probability of belonging to the *C. decresii* genetic cluster ($q \geq 0.90$; mean ± SD =
350 0.99 ± 0.02) with the exception of two admixed individuals ($q = 0.81$ and 0.57). All
351 individuals from the northernmost sites 9 – 14 had a high probability of belonging to the *C.*

352 *modestus* genetic cluster ($q \leq 0.10$; mean ± SD = 0.04 ± 0.03). Hybrids were identified within
353 sites 3 – 8 where all individuals were of mixed ancestry and exhibited a highly skewed
354 continuum of q-values ranging from 0.53 to 0.11. These sites will hereinafter be referred to as
355 'the contact zone', encompassing a distance of approximately 22.5 km. We also identified a
356 density trough of approximately 12 km between sites 2 and 3 (Figures 2c–d) across which the
357 genotype changes abruptly and multi-year surveys recovered no individuals. With the
358 exception of two individuals at site 3, all admixed individuals in sites 3 – 13 had *C. modestus*
359 mtDNA haplotypes. The *C. decresii* mtDNA haplotype was fixed in sites 1 – 2, including the
360 only two admixed individuals identified in the geographic range of *C. decresii* (Figure S3).
361 The first axis of the PCoA constructed from 1,333 loci clustered all populations into
362 two major groups corresponding to *C. modestus* and *C. decresii* (variance explained = 19.4%;
363 Figure 3). We found evidence for the presence of hybrids along this axis, with hybrids
364 clustered more closely to the Olary Ranges (OR) population of *C. modestus*. Population
365 pairwise measures of F_{ST} between the contact zone and *C. modestus* OR/SFR/NFR
366 populations (F_{ST} range: 0.058 – 0.216; Table S4) were lower relative to measures of F_{ST}
367 between the contact zone and *C. decresii* MS/KI populations (F_{ST} range: 0.203 – 0.293). The
368 contact zone had the lowest inbreeding coefficient (F = 0.095) and the highest level of
369 heterozygosity (H_{exp} = 0.084, H_{obs} = 0.079) relative to parental populations, with very similar
370 allelic number and richness to the OR population (Table 1). The second PCoA axis (variance
371 explained = 3.5%; Figure 3) showed population structure within each species, with the
372 Northern Flinders Ranges (NFR) and Kangaroo Island (KI) populations showing
373 differentiation from other populations of their respective species, and from each other (F_{ST} =
374 0.571; Table S4). This can likely be attributed to the fact that each represents the
375 northernmost and southernmost populations of their species, and KI is an insular population.

Hybrid classification

We found a strong bias in genetic introgression with admixed individuals being predominantly backcrossed with *C. modestus*. Of individuals within the contact zone, 35% had intermediate *q*-values ($0.4 < q < 0.6$) and a large proportion (65%) had *q*-values between 0.39 and 0.10 suggestive of backcrossing. NewHybrids analysis classified all individuals of *C. modestus* and *C. decresii* ($0.1 > q > 0.9$) as pure parental forms (PP ≥ 99.1%). Further, 59 of 79 individuals in the contact zone were classified to one of the six classes with a posterior probability (PP) of ≥ 95%. Additionally, 6 individuals were classified as pure *C. modestus* (P1), 36 as F2 hybrids, and 19 as backcrosses to the northern lineage (B1). We did not recover any F1 hybrids or backcrosses to *C. decresii*, posterior probabilities for these two categories were uniformly low (average PP = 0.0%). The two admixed individuals found in the geographic range of *C. decresii* were ambiguously classified as an F2 (PP = 54.2%) and a backcross to *C. decresii* (PP = 80.8%). The 22 individuals unable to be confidently classified (PP ≤ 95%) likely represent the continuum present in wild populations, unsuited for discrete classification, and difficult to distinguish even with many diagnostic markers (Boecklen & Howard, 1997; Vähä & Primmer, 2006).

Population history

The δaδi analysis showed that the model of secondary contact with ongoing asymmetrical migration ("sec_contact_asym_mig") was more likely than the model with subsequent isolation ("sec_contact_asym_mig_three_epoch"), based on log-likelihood and AIC (Figure S4, Table S5). To aid interpretation, we converted parameter estimates into biologically meaningful values (Figure 4; Figure S2). For the top model, the total time since divergence of *C. decresii* and *C. modestus* was ~1.95 million years (T1+T2), with secondary contact occurring ~170,000 years ago (T2). The 'population' size of *C. modestus* (Nu2) was

400 approximately 4 times larger than *C. decresii* (Nu1), and migration was asymmetrical with
401 0.36 individuals from *C. modestus* to *C. decresii* per generation compared to 1.55 individuals
402 from *C. decresii* to *C. modestus* per generation (Figure 4).

403 *Hybrid throat and dorsolateral phenotypes*

404 The throat phenotype of wild-caught hybrid males was more similar to that of *C.*
405 *modestus*, exhibiting all four throat colour morphs with uniformly low levels of UV
406 reflectance. Linear discriminant analyses (LDA) on throat variables showed *C. modestus* and
407 *C. decresii* strongly differentiated along LD1 which was driven primarily by the proportion of
408 blue and secondarily by QC_{UVS} and the proportion of orange (variance explained = 99.8%;
409 Figure 5a, Table S6). The 95% confidence ellipses drawn for the throat phenotypes of *C.*
410 *modestus* and hybrid males overlie each other. The large majority of hybrid throats cluster
411 with *C. modestus* throats. Blue coloration was not detected on the throats of pure *C. modestus*
412 males. A degree of blue coloration (≥ 5% blue pixels in segmentation analysis), however, was
413 found on a portion of hybrid throats of each morph: grey (47.4%, N = 19), orange (5.2%, N =
414 39), orange-yellow (6.7%, N = 15), yellow (11.8%, N = 17; Figure 6a). The throat phenotype
415 of the two hybrid individuals found in the range of *C. decresii* had larger proportions of blue
416 coloration on the throat relative to other hybrids.

417 In contrast to wild-caught hybrid throats, captive-bred F1 hybrid throat phenotype was
418 more intermediate and exhibited a wide range of UV reflectance levels varying from those
419 characteristic of *C. modestus* to *C. decresii*. Linear discriminant analysis on throat variables of
420 captive-bred F1 hybrids showed strong differentiation between lineages along LD1 driven
421 primarily by QC_{UVS} and secondarily by the proportions of blue and yellow (variance
422 explained = 88.0%; Figure 5b, Table S6). The 95% confidence ellipse drawn for hybrid
423 throats overlaps those of both *C. modestus* and *C. decresii* throats to a similar extent. Results

424 were essentially unchanged when considering hybrids sired by a *C. modestus* or *C. decresii*
425 male and by offspring sex. Similar to wild hybrids, all four *C. modestus* throat colour morphs
426 were recovered in captive-bred hybrids, and all but the orange-yellow morph had a proportion
427 of individuals with a blue component: grey (32.3%, N = 31), orange (18.5%, N = 27),
428 orange-yellow (0%, N = 2), yellow (8.3%, N = 12; Figure 6b). Although the artificial
429 elevation of testosterone levels has been shown to induce the expression of *C. modestus* throat
430 colour morphs in juveniles and females (Rankin et al., 2016; Rankin & Stuart-Fox, 2015), we
431 found that it did not comparably induce the expression of the blue throat colour morph in all
432 pure *C. decresii* offspring. Therefore, the presence of blue coloration on F1 hybrid offspring
433 throats may have been underestimated.

434 Dorsolateral phenotype in both wild-caught and captive-bred hybrids is intermediate
435 between the lineages (Figure 5c–d). Within the contact zone, differentiation between lineages
436 along LD1 is driven primarily by the number of breaks in the dorsolateral stripe and
437 proportion of orange (Table S6). The 95% confidence ellipses drawn for the dorsolateral
438 phenotypes of hybrids and *C. modestus* males overlap incompletely, likely reflecting the high
439 frequencies of backcrossing to *C. modestus*. In captive-bred hybrids, comparable results were
440 found with differentiation driven by breaks in the lateral stripe (Table S6) and the 95%
441 confidence ellipse for hybrid dorsolateral phenotype overlaps those of both *C. modestus* and
442 *C. decresii* dorsolateral phenotypes.

443 *Geographic clines*

444 Model-averaged clines for mtDNA and throat phenotype (QC_{UVS} and T_{PC1}) exhibited
445 relatively narrower clines with abrupt transitions suggesting selection on these traits,
446 compared to clines for the hybrid index (H_{Index}) and dorsolateral phenotype (D_{PC1}; Table 2).
447 The best-fitting clines for the hybrid index and mtDNA had coincident centres with

448 overlapping CIs but showed discordance in slope where the mtDNA cline was significantly
449 narrower (H_{Index}: c = 28.41 km, w = 29.77 km; mtDNA: c = 27.78 km, w = 0.64 km; Figure
450 8a–b). The cline fitted for the dorsolateral phenotype (c = 23.02 km, w = 13.97) was
451 coincident with that of the hybrid index (Figure 8c). Clines for throat phenotype (QC_{UVS} and
452 T_{PC1}) were similar in centre and width to each other (QC_{UVS}: c = 15.90 km, w = 8.48 km;
453 T_{PC1}: c = 15.38 km, w = 3.22 km; Figure 8d), their centres were displaced by 12.51 and 13.03
454 km to the south from the hybrid index cline centre and do not have overlapping CIs with the
455 hybrid index cline. See Table S7 for full details of cline models in the AIC 95% confidence
456 set for each trait.
457
458 **Discussion**
459 Evaluating the evolutionary outcomes of secondary contact between lineages that
460 differ in morph composition can provide valuable insights into the role of polymorphism in
461 speciation. We characterised genomic and phenotypic patterns across the contact zone
462 between the colour polymorphic *C. modestus* and monomorphic *C. decresii* and concurrently
463 measured the phenotype of captive-bred F1 hybrids. We found that the contact zone is
464 geographically narrow relative to the parental ranges (approx. 30 km) with no parental forms
465 or F1 hybrids present in the genetic centre, suggesting that hybridisation is neither recent nor
466 ongoing. Genomic introgression was asymmetric, with hybrids backcrossing almost
467 exclusively to *C. modestus*. Formal comparison of two plausible models of population history
468 for this system supports a prolonged period of secondary contact with asymmetrical
469 migration. This suggests that despite potential for admixture throughout the last interglacial
470 period, hybridisation between the species is not ongoing. Dorsolateral phenotype across the
471 contact zone was consistent with patterns of genetic admixture, whereas the cline for throat

472 phenotype was displaced relative to clines for the hybrid index and dorsolateral phenotype.
473 Throat phenotype of wild-caught hybrids resembled that of *C. modestus*, with all four *C.*
474 *modestus* throat morphs present and uniformly low UV reflectance. By contrast, both
475 dorsolateral and throat phenotype were intermediate in captive-bred F1 hybrids. Taken
476 together, these data are consistent with selection on throat phenotype across the contact zone.
477 The pattern of asymmetric genomic introgression, with limited backcrossing to the
478 southern lineage, could reflect multiple evolutionary and demographic scenarios. First,
479 extrinsic barriers may hinder dispersal and migration, in turn preventing backcrossing.
480 Second, the pattern of asymmetric genomic introgression coupled with the prevalence of *C.*
481 *modestus* mtDNA could potentially be explained by demographic circumstances. For
482 instance, a greater abundance of *C. modestus* individuals during initial periods of
483 hybridisation with continued asymmetric migration into the contact zone, or the sex-biased
484 dispersal of *C. decresii* males to the north, could both result in asymmetric introgression.
485 Third, intrinsic genomic incompatibilities could limit backcrossing via reinforcement (i.e.
486 selection against maladaptive hybridsation). We discuss each explanation below in light of
487 our data and available evidence.
488 The restricted gene flow to *C. decresii* is associated with an approximately 12 km
489 density trough (Figure 3b–c). In this region, it appears that hybrid and/or pure populations
490 either occur in levels below human detection or do not currently exist despite continuous
491 rocky habitat with no obvious barriers to dispersal (e.g. major roads, waterways, human
492 structures; Figure S5). The density trough was surveyed thoroughly in 2016 and 2017 and
493 briefly in 2013. The presence of suitable habitat was confirmed by surveys on foot, satellite
494 imagery (Figure S5), and/or flying drone surveys; this area is unlikely to constitute an
495 ecological barrier. Furthermore, a model with prolonged secondary contact and ongoing

496 asymmetric migration better fits the data than one with subsequent isolation. Secondary
497 contact over at least the last interglacial period suggests a sufficient period for dispersal across
498 the 12 km density trough in the absence of extrinsic barriers. Although dispersal has not been
499 examined in *C. decresii*, dispersal estimates in other lizard species range from 0.01 km/gen to
500 0.1 km/gen for Dactyloidae and Lacertidae (Calsbeek, Duryea, Parker, & Cox, 2014;
501 reviewed in McEntee et al., 2020; Vercken, Sinervo, & Clobert, 2012). With a generation
502 time of two years, dispersal across this distance is consistent with the estimated age of the
503 contact zone. In general, the width of the genetic contact zone (approx. 30 km), even taking
504 into consideration the 12 km density trough, is relatively narrow relative to the parental
505 ranges (Figure 2b). This distance is in accordance with cline widths estimated from genetic
506 data in other lizards: Teiidae (3.2 – 93.9 km; Dessauer, Cole, & Townsend, 2000; Gifford,
507 2008), Dactyloidae (3 – 5 km; Case & Williams, 1984; Johansson, Surget-Groba, & Thorpe,
508 2008), Lacertidae (2.7 – 29.9 km; Miraldo, Faria, Hewitt, Paulo, & Emerson, 2013),
509 Phrynosomatidae (0.8 – 30.9 km; Leaché & Cole, 2007; Leaché, Grummer, Harris, &
510 Breckheimer, 2017; J. C. Marshall & Sites Jr., 2001; Sites, Barton, & Reed, 1995).
511 Demographic factors alone are similarly unlikely to explain the observed asymmetric
512 introgression. The greater abundance and migration of *C. modestus* individuals into the
513 contact zone should result in a greater proportion of *C. modestus* genomic background (*C.*
514 *decresii* genomic signature quickly eroded by *C. modestus* contribution). However, we found
515 close to equal genomic proportions in many hybrids in the genetic centre. Despite opportunity
516 for ongoing migration, albeit asymmetrical, hybrids backcrossed to *C. decresii* were almost
517 entirely absent. Male-biased dispersal could underlie population genetic structure consistent
518 with our results (Jockusch & Wake, 2002; Petit & Excoffier, 2009); however, it is unlikely

519 that male-biased dispersal would exclusively be observed in *C. decresii* and not in *C.*
520 *modestus* given their polygynous mating systems (reviewed in Li & Kokko, 2019).
521 The absence of extrinsic barriers coupled with the narrower and more abrupt transition
522 exhibited by the mtDNA cline relative to the hybrid index, and the rarity of admixed
523 individuals containing the *C. decresii* mtDNA haplotype, point to a role for intrinsic genomic
524 incompatibilities (e.g. Helbig, Salomon, Bensch, & Seibold, 2001; Miller, Lipshutz, Smith, &
525 Bermingham, 2014). Captive breeding experiments between *C. modestus* and *C. decresii*
526 show no significant prezygotic barriers to the formation of F1 hybrids with either parental
527 mtDNA haplotype (Dong, Rankin, McLean, & Stuart-Fox, unpublished data), although their
528 reproductive viability is unknown. However, stronger incompatibilities and hybrid breakdown
529 are more frequently seen in F2 and later generation hybrids during the early stages of
530 divergence. This has been described extensively for both Dobzhansky-Muller
531 incompatibilities (reviewed in Coyne & Orr, 2004) and for cytonuclear incompatibilities
532 (Ellison & Burton, 2008; Fishman & Willis, 2006; Meiklejohn et al., 2013; Niehusis, Judson,
533 & Gadau, 2008). Overall, our results support the hypothesis that intrinsic factors contribute to
534 limiting gene flow, and backcrossing to *C. decresii*, regardless of mtDNA haplotype, may
535 result in offspring that are inviable, infertile, or suffer reduced fitness.
536 Phenotypic patterns recovered from within the contact zone could theoretically result
537 from selection on the throat colour signal or neutral processes. We found that both throat
538 phenotype clines were displaced relative to the genetic cline, in contrast to the dorsolateral
539 phenotype cline. The displaced throat phenotype clines and prevalence of the *C. modestus*
540 throat phenotype in the contact zone could theoretically arise from genetic dominance. In this
541 scenario, captive-bred F1 hybrids would be expected to have largely *C. modestus* throat
542 phenotypes which contrasts with the observed intermediate phenotypes. Another possibility is

543 that this phenotypic pattern is due to extensive backcrossing to *C. modestus*. While some wild
544 hybrids may have northern throat phenotypes because they are heavily backcrossed to *C.*
545 *modestus*, the prevalence of *C. modestus* phenotype in hybrids with close to equal proportions
546 of *C. modestus* and *C. decresii* genomic backgrounds points towards selection on throat
547 colour.

548 We did not detect the loss of any *C. modestus* throat morphs across the contact zone or
549 in F1 hybrids, indicating that co-adapted trait complexes of the *C. modestus* polymorphism
550 are stable despite genetic disruption. The maintenance of all four morphs in all populations of
551 *C. modestus* despite environmental selection on morph frequencies suggests that negative
552 frequency dependent selection is a strong evolutionary force counteracting loss of
553 polymorphism due to drift (McLean, Stuart-Fox, & Moussalli, 2015). Although hybrid throats
554 more closely resembled *C. modestus* throat morphs, we observed a proportion of each morph
555 which exhibited a degree of intermediate nature where an area of blue coloration was present.
556 There was a notably higher proportion of grey morphs which had blue coloration present.
557 This may be due to the similar mechanism by which grey and blue skin are produced in *C.*
558 *modestus* and *C. decresii* (McLean, Lutz, Rankin, Stuart-Fox, & Moussalli, 2017).
559 Nevertheless, we did not detect any hybrid throats that exhibited a true *C. decresii* throat
560 phenotype with both predominantly blue throat coloration and a high level of UV reflectance.
561 This, in addition to the variable presence of UV reflectance in captive-bred F1 hybrids, points
562 toward the uncoupling of blue coloration and UV reflectance in hybrids. Hybridisation can
563 generate novel phenotypes (e.g. blue without UV); for example, admixture between treefrog
564 lineages which have red and red/blue legs result in purple legs which are produced from the
565 directional introgression of colour loci inherited from parental lineages (Akopyan et al.,
566 2020).

567 Selection on throat coloration could be driven by mating behaviour which evolved via
568 reinforcement and/or microhabitat characteristics. Mate preference trials with captive *C.*
569 *modestus* and *C. decresii* predict a greater frequency of mating between *C. decresii* females
570 with *C. modestus* males than the reciprocal combination(McLean, Bartle, Dong, Rankin, &
571 Stuart-Fox, 2020). This contrasts with patterns observed within the contact zone, indicating
572 that prezygotic barriers between species have not evolved in allopatry. However, postzygotic
573 barriers (inferred from low frequency of hybrids backcrossed to the south) should select for
574 the formation of prezygotic barriers to prevent maladaptive hybridisation (i.e. reinforcement).
575 Extrinsic factors could also contribute to the *C. modestus* throat phenotype having a
576 competitive advantage in the contact zone, for example, due to a relatively higher
577 conspicuousness to conspecifics. The throat coloration of each species is more conspicuous
578 against the predominant background colours of native lichen in their respective ranges
579 (McLean, Moussalli, & Stuart-Fox, 2014). Within the contact zone, lichen coloration is
580 similar to that found in the range of *C. modestus*, predominantly pale green. Therefore, sexual
581 selection may operate through male-male interactions or female choice to result in a
582 reproductive advantage of the *C. modestus* throat phenotype as a more conspicuous and
583 detectable visual signal (reviewed in Servedio & Boughman, 2017). Similarly, the greater
584 overlap of hybrid phenotype (e.g. ventral coloration) with one parental species was associated
585 with environmental variation in *Hyperolius* frogs (Bell & Irian, 2019). Selection has been
586 shown to drive the rapid spread of an advantageous trait/phenotype across contact zones, and
587 in some cases into the other parental lineage (Baldassarre, White, Karubian, & Webster, 2014;
588 Pardo-Diaz et al., 2012; Stein & Uy, 2006; While et al., 2015). In contrast, the dorsolateral
589 phenotype cline indicates that it is not under similarly strong selection and appears to play a
590 lesser role in reproductive isolation in sympatry. Male dorsolateral coloration may be

591 constrained as it is under both sexual and natural selection because of its dual function as a
592 intraspecific signal and in minimising conspicuousness to predators against native lichen
593 (McLean, Moussalli, et al., 2014; Ramos & Peters, 2016).

594 *Conclusions*

595 In summary, our study suggests that sexual signal divergence and intrinsic genetic
596 incompatibilities play an important role in restricting gene flow between the polymorphic *C.*
597 *modestus* and monomorphic *C. decresii*. The species remain distinct despite continued
598 migration and opportunity for gene flow. The stability of the *C. modestus* polymorphism
599 despite genetic disruption is consistent with the theoretical genetic architecture of colour
600 polymorphism and correlated traits, namely control by pleiotropic or tightly linked genes.
601 Taken together, these results lend support to the view that polymorphism can promote
602 speciation.

603

604 **Acknowledgements**

605 This study was funded by the Australian Research Council (DP150101048 and DP1092908)
606 to D.S-F., Holsworth Wildlife Endowment and The David Lachlan Hay Memorial Fund to
607 C.M.D., and Holsworth Wildlife Endowment, Alfred Nicholas Fellowship and Nature
608 Foundation South Australia to C.A.M. We thank Madeleine Yewers, Steven Mesis, Katrina
609 Rankin and Anne Auslebrook for assistance; private landowners for kindly allowing land
610 access; and South Australian Museum for providing tissue samples. Data collection was
611 conducted with permits from the Department of Environment, Water and Natural Resources,
612 South Australia (permit nos. E25861-1 and Q26428-3), the Department of Environment,
613 Land, Water and Planning, Victoria (permit nos. 10007000 and 10007751) and with approval
614 by The University of Melbourne Animals Ethics Committee (approval nos. 1011760.1 and

1413220.4), the Wildlife Ethics Committee of South Australia (approval nos. 18/2010 and 25/2015). We thank Ben Phillips and three anonymous reviewers for insightful comments, which helped to improve the manuscript.

References

Akopyan, M., Gompert, Z., Klonoski, K., Vega, A., Kaiser, K., Mackelprang, R., … Robertson, J. M. (2020). Genetic and phenotypic evidence of a contact zone between divergent colour morphs of the iconic red-eyed treefrog. *Molecular Ecology*, 1–15. doi: 10.1111/mec.15639

Anderson, E. C., & Thompson, E. A. (2002). A model-based method for identifying species hybrids using multilocus genetic data. *Genetics*, *160*(3), 1217–1229.

Baldassarre, D. T., White, T. A., Karubian, J., & Webster, M. S. (2014). Genomic and morphological analysis of a semipermeable avian hybrid zone suggests asymmetrical introgression of a sexual signal. *Evolution*, *68*(9), 2644–2657. doi: 10.1111/evo.12457

Bartoń, K. (2018). *MuMIn: Multi-Model Inference. R package version 1.42.1. https://CRAN.R-project.org/package=MuMIn*.

Bell, R. C., & Irian, C. G. (2019). Phenotypic and genetic divergence in reed frogs across a mosaic hybrid zone on São Tomé Island. *Biological Journal of the Linnean Society*, *128*(3), 672–680. doi: 10.1093/biolinnean/blz131

Boecklen, W. J., & Howard, D. J. (1997). Genetic analysis of hybrid zones: numbers of markers and power of resolution. *Ecology*, *78*(8), 2611–2616.

Boughman, J. W. (2001). Divergent sexual selection enhances reproductive isolation in sticklebacks. *Nature*, *411*(6840), 944–948. doi: 10.1038/35082064

Burnham, K., & Anderson, D. (2002). *Model selection and multimodel inference* (2nd ed.). New York: Springer.

Burton, R. S., & Barreto, F. S. (2012). A disproportionate role for mtDNA in Dobzhansky-Muller incompatibilities? *Molecular Ecology*, *21*(20), 4942–4957. doi: 10.1111/mec.12006

Byrne, M. (2008). Evidence for multiple refugia at different time scales during Pleistocene climatic oscillations in southern Australia inferred from phylogeography. *Quaternary Science Reviews*, *27*, 2576–2585. doi: 10.1016/j.quascirev.2008.08.032

Calsbeek, R., Duryea, M. C., Parker, E., & Cox, R. M. (2014). Sex-biased juvenile dispersal is adaptive but does not create genetic structure in island lizards. *Behavioral Ecology*, *25*(5), 1157–1163. doi: 10.1093/beheco/aru102

Case, S. M., & Williams, E. E. (1984). Study of a Contact Zone in the Anolis distichus Complex in the Central Dominican Republic. *Herpetologica*, *40*(2), 118–137.

Clement, M., Posada, D., & Crandall, K. A. (2000). TCS: a computer program to estimate gene genealogies. *Molecular Ecology*, *9*(10), 1657–1659. doi: 10.1046/j.1365-

294x.2000.01020.x

Corl, A., Davis, A. R., Kuchta, S. R., & Sinervo, B. (2010). Selective loss of polymorphic mating types is associated with rapid phenotypic evolution during morphic speciation. *Proceedings of the National Academy of Sciences*, *107*(9), 4254–4259. doi: 10.1073/pnas.0909480107

Coyne, J. A., & Orr, H. A. (2004). Speciation. In *Sinauer Associates*. Sunderland, Massachusetts: Sinauer Associates.

Derryberry, E. P., Derryberry, G. E., Maley, J. M., & Brumfield, R. T. (2014). HZAR: hybrid zone analysis using an R software package. *Molecular Ecology Resources*, *14*(3), 652–663. doi: 10.1111/1755-0998.12209

Dessauer, H. C., Cole, C. J., & Townsend, C. R. (2000). Hybridization among western whiptail lizards (Cnemidophorus tigris) in Southwestern New Mexico: Population genetics, morphology, and ecology in three contact zones. *Bulletin of the American Museum of Natural History*, (246), 1–127.

Dobzhansky, T. (1937). Genetics the Origin and of Species. In *Genetics and the origin of species*. New York: Columbia University Press.

Dong, C. M., Johnston, G. R., Stuart-Fox, D., Moussalli, A., Rankin, K. J., & McLean, C. A. (2021). Elevation of divergent color polymorphic and monomorphic lizard lineages (Squamata: Agamidae) to species level. *Ichthyology and Herpetology*, *109*(1). doi: 10.1643/h2020064

Earl, D. A., & VonHoldt, B. M. (2012). STRUCTURE HARVESTER: a website and program for visualizing STRUCTURE output and implementing the Evanno mothod. *Conservation Genetics Resources*, *4*(2), 359–360. doi: 10.1007/s12686-011-9548-7

Ellison, C. K., & Burton, R. S. (2008). Interpopulation hybrid breakdown maps to the mitochondrial genome. *Evolution*, *62*(3), 631–638. doi: 10.1111/j.1558-5646.2007.00305.x

Fishman, L., & Willis, J. H. (2006). A cytonuclear incompatibility causes anther sterility in *Mimulus* hybrids. *Evolution*, *60*(7), 1372–1381. doi: 10.1554/05-708.1

Forsman, A., Ahnesjö, J., Caesar, S., & Karlsson, M. (2008). A model of ecological and evolutionary consequences of color polymorphism. *Ecology*, *89*(1), 34–40. doi: 10.1890/07-0572.1

Forstner, M. R., Davis, S. K., & Arèvalo, E. (1995). Support for the hypothesis of anguimorph ancestry for the suborder Serpentes from phylogenetic analysis of mitochondrial DNA sequences. *Molecular Phylogenetics and Evolution*, *4*(1), 93–102. doi: 10.1006/mpev.1995.1010

Gay, L., Crochet, P. A., Bell, D. A., & Lenormand, T. (2008). Comparing clines on molecular and phenotypic traits in hybrid zones: A window on tension zone models. *Evolution*, *62*(11), 2789–2806. doi: 10.1111/j.1558-5646.2008.00491.x

Georges, A., Li, Q., Lian, J., O'Meally, D., Deakin, J., Wang, Z., … Zhang, G. (2015). High-coverage sequencing and annotated assembly of the genome of the Australian dragon lizard *Pogona vitticeps*. *GigaScience*, *4*(1), 45. doi: 10.1186/s13742-015-0085-2

Gibbons, J. R. H. (1977). *Comparative ecology and behaviour of lizards of the* Amphibolurus decresii *species complex*. The University of Adelaide.

Gibbons, J. R. H. (1979). The hind leg pushup display of the *Amphibolurus decresii* species complex (Lacertilia: Agamidae). *Copeia*, *1*, 29–40. doi: 10.2307/1443725

Gifford, M. E. (2008). Divergent character clines across a recent secondary contact zone in a Hispaniolan lizard. *Journal of Zoology*, *274*(3), 292–300. doi: 10.1111/j.1469-7998.2007.00385.x

Gosselin, T., Lamothe, M., Devloo-Delva, F., & Grewe, P. (2020). *radiator: RADseq Data Exploration, Manipulation and Visualization using R*. doi: 10.5281/zenodo.3687060

Gray, S. M., & McKinnon, J. S. (2007). Linking color polymorphism maintenance and speciation. *Trends in Ecology & Evolution*, *22*(2), 71–79. doi: 10.1016/j.tree.2006.10.005

Gruber, B., Unmack, P. J., Berry, O. F., & Georges, A. (2018). dartR: An R package to facilitate analysis of SNP data generated from reduced representation genome sequencing. *Molecular Ecology Resources*, *18*, 691–699. doi: 10.1111/1755-0998.12745

Gutenkunst, R., Hernandez, R., Williamson, S., & Bustamante, C. (2009). Inferring the joint demographic history of multiple populations from multidimensional SNP frequency data. *PLoS Genetics*, *5*(10). doi: 10.1371/journal.pgen.1000695

Gutenkunst, R., Hernandez, R., Williamson, S., & Bustamante, C. (2010). Diffusion approximations for demographic inference: DaDi. *Nature Precedings*. doi: 10.1038/npre.2010.4594.1

Hacking, J. D., Stuart-Fox, D., Godfrey, S. S., & Gardner, M. G. (2018). Specific MHC class I supertype associated with parasite infection and color morph in a wild lizard population. *Ecology and Evolution*, *8*(19), 9920–9933. doi: 10.1002/ece3.4479

Helbig, A. J., Salomon, M., Bensch, S., & Seibold, I. (2001). Male-biased gene flow across an avian hybrid zone: Evidence from mitochondrial and microsatellite DNA. *Journal of Evolutionary Biology*, *14*(2), 277–287. doi: 10.1046/j.1420-9101.2001.00273.x

Hill, G. E. (2015). Mitonuclear ecology. *Molecular Biology and Evolution*, *32*(8), 1917–1927. doi: 10.1093/molbev/msv104

Hooper, D. M., Griffith, S. C., & Price, T. D. (2019). Sex chromosome inversions enforce reproductive isolation across an avian hybrid zone. *Molecular Ecology*, *28*(6), 1246–1262. doi: 10.1111/mec.14874

Houston, T. F. (1974). Revision of the *Amphibolurus decresii* complex (Lacertilia: Agamidae) of South Australia. *Transactions of The Royal Society of South Australia*, *98*(2), 49–60. doi: 10.1126/science.97.2526.482-a

Hugall, A. F., & Stuart-Fox, D. (2012). Accelerated speciation in colour-polymorphic birds. *Nature*, *485*, 631–634. doi: 10.1038/nature11050

Huxley, J. (1955). Morphism in birds. *Acta International Congress Ornithology XI*, 309–328.

Jakobsson, M., & Rosenberg, N. A. (2007). CLUMPP: A cluster matching and permutation

program for dealing with label switching and multimodality in analysis of population structure. *Bioinformatics*, *23*(14), 1801–1806. doi: 10.1093/bioinformatics/btm233

Jiggins, C. D., Naisbit, R. E., Coe, R. L., & Mallet, J. (2001). Reproductive isolation caused by colour pattern mimicry. *Nature*, *411*(6835), 302–305. doi: 10.1038/35077075

Jockusch, E. L., & Wake, D. B. (2002). Falling apart and merging: Diversification of slender salamanders (Plethodontidae: Batrachoseps) in the American West. *Biological Journal of the Linnean Society*, *76*(3), 361–391. doi: 10.1046/j.1095-8312.2002.00071.x

Johansson, H., Surget-Groba, Y., & Thorpe, R. S. (2008). The roles of allopatric divergence and natural selection in quantitative trait variation across a secondary contact zone in the lizard Anolis roquet. *Molecular Ecology*, *17*(23), 5146–5156. doi: 10.1111/j.1365-294X.2008.03979.x

Jombart, T., & Ahmed, I. (2011). adegenet 1.3-1: New tools for the analysis of genome-wide SNP data. *Bioinformatics*, *27*(21), 3070–3071. doi: 10.1093/bioinformatics/btr521

Kalinowski, S. T., Taper, M. L., & Marshall, T. C. (2007). Revising how the computer program CERVUS accommodates genotyping error increases success in paternity assignment. *Molecular Ecology*, *16*(5), 1099–1106. doi: 10.1111/j.1365-294X.2007.03089.x

Kearse, M., Moir, R., Wilson, A., Stones-havas, S., Sturrock, S., Buxton, S., … Drummond, A. (2012). Geneious Basic: An integrated and extendable desktop software platform for the organization and analysis of sequence data. *Bioinformatics*, *28*(12), 1647–1649. doi: 10.1093/bioinformatics/bts199

Kilian, A., Wenzl, P., Huttner, E., Carling, J., Xia, L., Caig, V., … Uszynski, G. (2012). Diversity Arrays Technology: A Generic Genome Profiling Technology on Open Platforms. In F. Pompanon & A. Bonin (Eds.), *Data Production and Analysis in Population Genomics. Methods in Molecular Biology (Methods and Protocols)* (Vol. 888, pp. 67–89). doi: 10.1007/978-1-61779-870-2

Lê, S., Josse, J., & Husson, F. F. (2008). FactoMineR: An R Package for Multivariate Analysis. *Journal of Statistical Software*, *25*(1), 1–18. doi: 10.1016/j.envint.2008.06.007

Leaché, A. D., & Cole, C. J. (2007). Hybridization between multiple fence lizard lineages in an ecotone: Locally discordant variation in mitochondrial DNA, chromosomes, and morphology. *Molecular Ecology*, *16*(5), 1035–1054. doi: 10.1111/j.1365-294X.2006.03194.x

Leaché, A. D., Grummer, J. A., Harris, R. B., & Breckheimer, I. K. (2017). Evidence for concerted movement of nuclear and mitochondrial clines in a lizard hybrid zone. *Molecular Ecology*, *26*(8), 2306–2316. doi: 10.1111/mec.14033

Li, X. Y., & Kokko, H. (2019). Sex-biased dispersal: a review of the theory. *Biological Reviews*, *94*(2), 721–736. doi: 10.1111/brv.12475

Lukacs, P. M., Burnham, K. P., & Anderson, D. R. (2010). Model selection bias and Freedman's paradox. *Annals of the Institute of Statistical Mathematics*, *62*(1), 117–125. doi: 10.1007/s10463-009-0234-4

Marshall, J. C., & Sites Jr., J. W. (2001). A comparison of nuclear and mitochondrial cline

shapes in a hybrid zone in the Sceloporus grammicus complex (Squamata ; Phrynosomatidae). *Molecular Ecology*, *10*, 435–449.

Marshall, T. C., Slate, J., Kruuk, L. E. B., & Pemberton, J. M. (1998). Statistical confidence for likelihood-based paternity inference in natural populations. *Molecular Ecology*, *7*, 639–655.

Mavárez, J., Salazar, C. A., Bermingham, E., Salcedo, C., Jiggins, C. D., & Linares, M. (2006). Speciation by hybridization in *Heliconius* butterflies. *Nature*, *441*(7095), 868–871. doi: 10.1038/nature04738

McEntee, J. P., Burleigh, J. G., & Singhal, S. (2020). Dispersal predicts hybrid zone widths across animal diversity: Implications for species borders under incomplete reproductive isolation. *American Naturalist*, *196*(1), 9–28. doi: 10.1086/709109

McLean, C. A., Bartle, R. A., Dong, C. M., Rankin, K. J., & Stuart-Fox, D. (2020). Divergent male and female mate preferences do not explain incipient speciation between lizard lineages. *Current Zoology*, (March), 1–8. doi: 10.1093/cz/zoaa010

McLean, C. A., Lutz, A., Rankin, K. J., Stuart-Fox, D., & Moussalli, A. (2017). Revealing the biochemical and genetic basis of color variation in a polymorphic lizard. *Molecular Biology and Evolution*, *34*(8), 1924–1935. doi: 10.1093/molbev/msx136

McLean, C. A., Moussalli, A., Sass, S., & Stuart-Fox, D. (2013). Taxonomic assessment of the *Ctenophorus decresii* complex (Reptilia: Agamidae) reveals a new species of dragon lizard from western New South Wales. *Records of the Australian Museum*, *65*(3), 51–63. doi: 10.3853/j.2201-4349.65.2013.1600

McLean, C. A., Moussalli, A., & Stuart-Fox, D. (2014). Local adaptation and divergence in colour signal conspicuousness between monomorphic and polymorphic lineages in a lizard. *Journal of Evolutionary Biology*, *27*(12), 2654–2664. doi: 10.1111/jeb.12521

McLean, C. A., & Stuart-Fox, D. (2014). Geographic variation in animal colour polymorphisms and its role in speciation. *Biological Reviews*, *89*(4), 860–873. doi: 10.1111/brv.12083

McLean, C. A., Stuart-Fox, D., & Moussalli, A. (2014). Phylogeographic structure, demographic history and morph composition in a colour polymorphic lizard. *Journal of Evolutionary Biology*, *27*(10), 2123–2137. doi: 10.1111/jeb.12464

McLean, C. A., Stuart-Fox, D., & Moussalli, A. (2015). Environment, but not genetic divergence, influences geographic variation in colour morph frequencies in a lizard. *BMC Evolutionary Biology*, *15*(1), 156. doi: 10.1186/s12862-015-0442-x

Meiklejohn, C. D., Holmbeck, M. A., Siddiq, M. A., Abt, D. N., Rand, D. M., & Montooth, K. L. (2013). An incompatibility between a mitochondrial tRNA and its nuclear-encoded tRNA synthetase compromises development and fitness in *Drosophila*. *PLoS Genetics*, *9*(1), e1003238. doi: 10.1371/journal.pgen.1003238

Melville, J., Haines, M. L., Boysen, K., Hodkinson, L., Kilian, A., Smith Date, K. L., … Parris, K. M. (2017). Identifying hybridization and admixture using SNPs: application of the DArTseq platform in phylogeographic research on vertebrates. *Royal Society Open Science*, *4*, 161061. doi: 10.1098/rsos.161061

Miller, M. J., Lipshutz, S. E., Smith, N. G., & Bermingham, E. (2014). Genetic and phenotypic characterization of a hybrid zone between polyandrous Northern and Wattled Jacanas in Western Panama. *BMC Evolutionary Biology*, *14*(1), 1–14. doi: 10.1186/s12862-014-0227-7

Miraldo, A., Faria, C., Hewitt, G. M., Paulo, O. S., & Emerson, B. C. (2013). Genetic analysis of a contact zone between two lineages of the ocellated lizard (*Lacerta lepida* Daudin 1802) in south-eastern Iberia reveal a steep and narrow hybrid zone. *Journal of Zoological Systematics and Evolutionary Research*, *51*(1), 45–54. doi: 10.1111/jzs.12005

Muller, H. J. (1942). Isolating mechanisms, evolution, and temperature. *Biol Symp*, *6*, 71–125.

Niehuis, O., Judson, A. K., & Gadau, J. (2008). Cytonuclear genic incompatibilities cause increased mortality in male F2 hybrids of *Nasonia giraulti* and *N. vitripennis*. *Genetics*, *178*(1), 413–426. doi: 10.1534/genetics.107.080523

Osborne, L., Umbers, K. D. L., Backwell, P. R. Y., & Keogh, J. S. (2012). Male tawny dragons use throat patterns to recognize rivals. *Naturwissenschaften*, *99*(10), 869–872. doi: 10.1007/s00114-012-0968-3

Pardo-Diaz, C., Salazar, C., Baxter, S. W., Merot, C., Figueiredo-Ready, W., Joron, M., … Jiggins, C. D. (2012). Adaptive introgression across species boundaries in *Heliconius* butterflies. *PLoS Genetics*, *8*(6), e1002752. doi: 10.1371/journal.pgen.1002752

Petit, R. J., & Excoffier, L. (2009). Gene flow and species delimitation. *Trends in Ecology and Evolution*, *24*(7), 386–393. doi: 10.1016/j.tree.2009.02.011

Portik, D. M., Leaché, A. D., Rivera, D., Barej, M. F., Burger, M., Hirschfeld, M., … Fujita, M. K. (2017). Evaluating mechanisms of diversification in a Guineo-Congolian tropical forest frog using demographic model selection. *Molecular Ecology*, *26*(19), 5245–5263. doi: 10.1111/mec.14266

Pritchard, J. K., Stephens, M., & Donnelly, P. (2000). Inference of population structure using multilocus genotype data. *Genetics*, *155*(2), 945–959. doi: 10.1111/j.1471-8286.2007.01758.x

Pryke, S. R., & Griffith, S. C. (2009). Postzygotic genetic incompatibility between sympatric color morphs. *Evolution*, *63*(3), 793–798. doi: 10.1111/j.1558-5646.2008.00584.x

Ramos, J. A., & Peters, R. A. (2016). Dragon wars: Movement-based signalling by Australian agamid lizards in relation to species ecology. *Austral Ecology*, *41*, 302–315. doi: 10.1111/aec.12312

Rankin, K. J., McLean, C. A., Kemp, D. J., & Stuart-Fox, D. (2016). The genetic basis of discrete and quantitative colour variation in the polymorphic lizard, *Ctenophorus decresii*. *BMC Evolutionary Biology*, *16*(1), 1–14. doi: 10.1186/s12862-016-0757-2

Rankin, K. J., & Stuart-Fox, D. (2015). Testosterone-induced expression of male colour morphs in females of the polymorphic tawny dragon lizard, *Ctenophorus decresii*. *PLOS ONE*, *10*(10), e0140458. doi: 10.1371/journal.pone.0140458

Sætre, G. P., Moum, T., Bureš, S., Král, M., Adamjan, M., Moreno, J., … Moreno, J. (1997). A sexually selected character displacement in flycatchers reinforces premating isolation.

Nature, *387*(June), 589–592. doi: 10.1038/42451

Schwartz, T. S., Warner, D. A., Beheregaray, L. B., Olsson, M., & Note, P. (2007). Microsatellite loci for Australian agamid lizards. *Molecular Ecology Notes*, *7*(3), 528–531. doi: 10.1111/j.1471-8286.2006.01644.x

Scott, I. A. W. W., & Keogh, J. S. (2000). Conservation genetics of the endangered grassland earless dragon *Tympanocryptis pinguicolla* (Reptilia: Agamidae) in Southeastern Australia. *Conservation Genetics*, *1*(4), 357–363. doi: 10.1023/A:1011542717349

Seehausen, O., Terai, Y., Magalhaes, I. S., Carleton, K. L., Mrosso, H. D. J., Miyagi, R., … Okada, N. (2008). Speciation through sensory drive in cichlid fish. *Nature*, *455*(7213), 620–627. doi: 10.1038/nature07285

Servedio, M. R., & Boughman, J. W. (2017). The role of sexual selection in local adaptation and speciation. *Annual Review of Ecology, Evolution, and Systematics*, *48*(1), 85–109. doi: 10.1146/annurev-ecolsys-110316-022905

Sinervo, B., & Svensson, E. (2002). Correlational selection and the evolution of genomic architecture. *Heredity*, *89*(5), 329–338. doi: 10.1038/sj.hdy.6800148

Singhal, S., & Moritz, C. (2013). Reproductive isolation between phylogeographic lineages scales with divergence. *Proceedings of the Royal Society B: Biological Sciences*, *280*, 20132246. doi: 10.1098/rspb.2013.2246

Sites, J. W., Barton, N. H., & Reed, K. M. (1995). The genetic structure of a hybrid zone between two chromosome races of the *Sceloporus grammicus* complex (Sauria, Phrynosomatidae) in central Mexico. *Evolution*, *49*(1), 9–36. doi: 10.1111/j.1558-5646.1995.tb05955.x

Stein, A. C., & Uy, J. A. C. (2006). Unidirectional introgression of a sexually selected trait across an avian hybrid zone: a role for female choice? *Evolution*, *60*(7), 1476–1485. doi: 10.1111/j.0014-3820.2006.tb01226.x

Stuart-Fox, D. M., & Johnston, G. R. (2005). Experience overrides colour in lizard contests. *Behaviour*, *142*, 329–350. doi: 10.1163/1568539053778265

Symonds, M. R. E., & Moussalli, A. (2011). A brief guide to model selection, multimodel inference and model averaging in behavioural ecology using Akaike's information criterion. *Behavioral Ecology and Sociobiology*, *65*, 13–21. doi: 10.1007/s00265-010-1037-6

Szymura, J. M., & Barton, N. H. (1986). Genetic analysis of a hybrid zone between the fire-bellied toads, *Bombina bombina* and *B . variegata*, near Cracow in Southern Poland. *Evolution*, *40*(6), 1141–1159.

Szymura, J. M., & Barton, N. H. (1991). The genetic structure of the hybrid zone between the fire-bellied toads *Bombina bombina* and *B. variegata*: comparisons between transects and between loci. *Evolution*, *45*(2), 237–261. doi: 10.1111/j.1558-5646.1991.tb04400.x

Teasdale, L. C., Stevens, M., & Stuart-Fox, D. (2013). Discrete colour polymorphism in the tawny dragon lizard (*Ctenophorus decresii*) and differences in signal conspicuousness among morphs. *Journal of Evolutionary Biology*, *26*(5), 1035–1046. doi: 10.1111/jeb.12115

Vähä, J. P., & Primmer, C. R. (2006). Efficiency of model-based Bayesian methods for detecting hybrid individuals under different hybridization scenarios and with different numbers of loci. *Molecular Ecology*, *15*(1), 63–72. doi: 10.1111/j.1365-294X.2005.02773.x

Venables, W. N., & Ripley, B. D. (2002). *Modern Applied Statistics with S* (Fourth). Retrieved from http://www.stats.ox.ac.uk/pub/MASS4

Vercken, E., Sinervo, B., & Clobert, J. (2012). The importance of a good neighborhood: Dispersal decisions in juvenile common lizards are based on social environment. *Behavioral Ecology*, *23*(5), 1059–1067. doi: 10.1093/beheco/ars075

West-Eberhard, M. J. (1986). Alternative adaptations, speciation, and phylogeny (A Review). *Proceedings of the National Academy of Sciences*, *83*, 1388–1392. doi: 10.1073/pnas.83.5.1388

While, G. M., Michaelides, S., Heathcote, R. J. P., Macgregor, H. E. A., Zajac, N., Beninde, J., … Uller, T. (2015). Sexual selection drives asymmetric introgression in wall lizards. *Ecology Letters*, *18*(12), 1366–1375. doi: 10.1111/ele.12531

Wringe, B. F., Stanley, R. R. E., Jeffery, N. W., Anderson, E. C., & Bradbury, I. R. (2017). parallelnewhybrid: an R package for the parallelization of hybrid detection using newhybrids. *Molecular Ecology Resources*, *17*(1), 91–95. doi: 10.1111/1755-0998.12597

Yewers, M. S. C., Jessop, T. S., & Stuart-Fox, D. (2017). Endocrine differences among colour morphs in a lizard with alternative behavioural strategies. *Hormones and Behavior*, *93*, 118–127. doi: 10.1016/j.yhbeh.2017.05.001

Yewers, M. S. C., Pryke, S. R., & Stuart-Fox, D. (2016). Behavioural differences across contexts may indicate morph-specific strategies in the lizard *Ctenophorus decresii*. *Animal Behaviour*, *111*, 329–339. doi: 10.1016/j.anbehav.2015.10.029

Data Accessibility

The DArTseq genotype data, mtDNA alignment, R code and morphological data that support the findings of this study are openly available in Dryad at http://doi.org[doi], reference number [number]. All mtDNA sequences are deposited in GenBank, accession numbers MW261595 - MW261739.

Data will be made available on Dryad upon acceptance of the manuscript.

Author Contributions

All authors contributed to study design and field sampling. C.M.D. and C.A.M. performed laboratory work. C.M.D. conducted data analyses and drafted the manuscript. C.A.M, A.M. and D.S-F provided input on analyses, interpretation, and the manuscript. All authors read and approved the final manuscript.

935 **Tables**
936

937 **Table 1.** Populations sampled across the ranges of *C. modestus* (Northern Flinders Ranges
938 [NFR), Southern Flinders Ranges [SFR], Olary Ranges [OR]), *C. decresii* (Mainland South
939 [MS], and Kangaroo Island [KI]), and Contact Zone (CZ), with details of sample size for the
940 SNP dataset (*N*), expected and observed heterozygosity (H_{exp}, H_{obs}), inbreeding coefficient
941 (F), allele number (AN), and allelic richness (AR).
942

Population	*N* (♂ / ♀ / NA)	H_{exp}	H_{obs}	F	AN	AR
NFR	7 (2 / 0 / 5)	0.064	0.055	0.177	1629	0.222
SFR	41 (31 / 8 / 2)	0.076	0.070	0.129	2091	0.569
OR	60 (45 / 7 / 8)	0.072	0.060	0.177	2138	0.604
CZ	82 (69 / 13 / 0)	0.084	0.079	0.095	2134	0.601
MS	33 (26 / 4 / 3)	0.051	0.043	0.175	1714	0.286
KI	7 (6 / 1 / 0)	0.023	0.019	0.165	1429	0.072
Total	230					

943 †Sex was unknown for a portion of loaned museum tissue samples.

944

Table 2. Model-averaged estimates for cline centre and width based on the AIC 95% confidence set models, with *N* representing the number of models within the AIC confident set. Cline centre is the distance (km) from the southern-most sampling site and width (*w*) is 1/slope at the centre. Two log-likelihood unit support limits are shown as 'low' and 'high'. See Table S7 for full details of cline models.

Trait		*N*	Centre	(low – high)	Width	(low – high)
Hybrid Index (H_{Index})		10	28.41	(22.37 – 33.00)	29.77	(15.05 – 55.84)
mtDNA		7	27.78	(14.59 – 28.17)	0.64	(0.08 – 21.85)
Dorsolateral Phenotype (D_{PC1})		2	23.02	(16.33 – 27.61)	13.97	(0.82 – 29.02)
Throat Phenotype	QC_{UVS}	4	15.90	(14.25 – 20.48)	8.48	(0.74 – 17.27)
	T_{PC1}	2	15.38	(15.06 – 16.61)	3.22	(2.43 – 7.94)

Figures

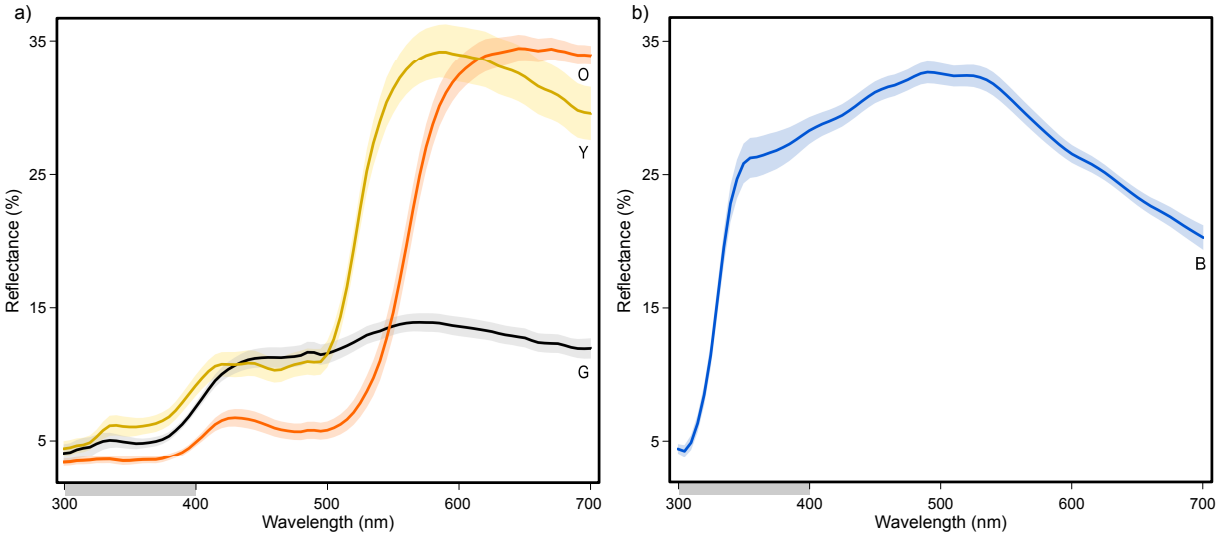

Figure 1. Average spectral reflectances of male throat colours found in (a) *C. modestus* measured from Southern Flinders Ranges populations: orange (O), yellow (Y), grey (G), and (b) *C. decresii* ultra-violet blue throat colour measured from Mainland South populations. Standard error shown as shaded region (N = 10 for each colour). Ultraviolet wavelengths are shown with a grey bar on the *x*-axis.

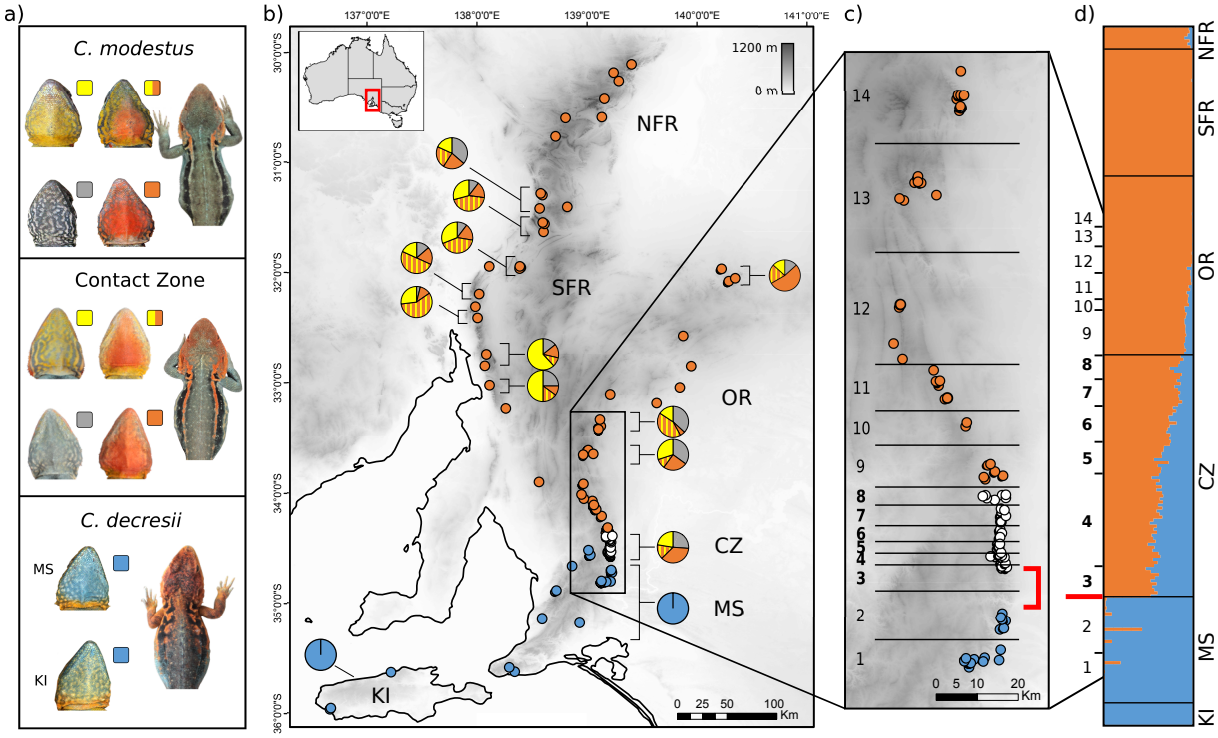

Figure 2. Geographic variation in throat colour morphs and genetic structure between *C. modestus* and *C. decresii*. (a) Representative throats (*C. modestus*: yellow, orange-yellow, grey and orange; *C. decresii*: blue) and dorsolateral phenotypes found in each species and the contact zone. (b) Map showing sampling localities of individuals used in genetic analyses: *C. modestus* (orange circles; Northern Flinders Ranges [NFR], Southern Flinders Ranges [SFR], Olary Ranges [OR]), *C. decresii* (blue circles; Mainland South [MS], and Kangaroo Island [KI]), and genetically admixed individuals (white circles; $0.1 < q < 0.9$). Pie charts indicate relative frequencies of male throat colour morphs. Proportions for the Southern Flinders Ranges and northernmost population in the Olary Ranges are adapted from McLean, Stuart-Fox, & Moussalli, 2015. Throat colour morph data are not available for the Northern Flinders Ranges. Elevation in meters is represented by grey shading on the scale bar. (c) An enlarged map section showing sites across the contact zone transect used for geographic cline analyses; (d) Results of a Bayesian analysis of ancestry in the program STRUCTURE (K = 2). Each horizontal bar represents an individual and individuals are ordered by latitude and population. The proportion of orange and blue represents the proportion of *C. modestus* and *C. decresii* ancestry in each individual. A density trough between sites 2 and 3, where surveys did not recover any individuals, is indicated in red in panels B and C.

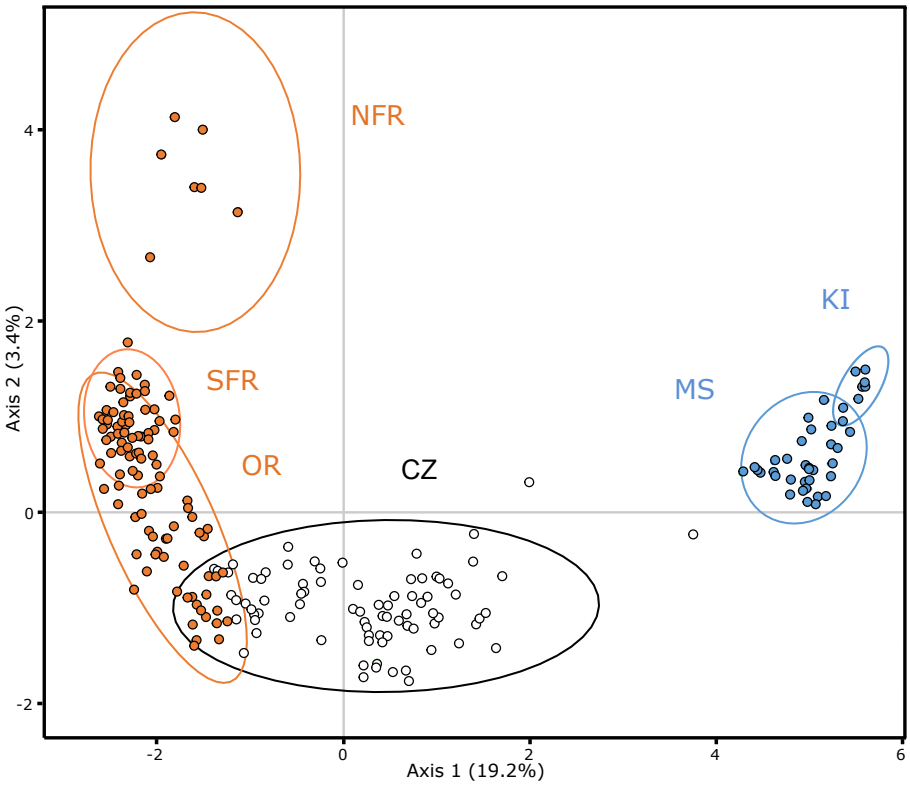

Figure 3. Two-dimensional principal coordinate plot (PCoA) constructed from the SNP data set (1,333 loci) showing pairwise genetic distances between individuals. 95% confidence ellipses of each group are shown (*C. modestus:* Northern Flinders Ranges [NFR], Southern Flinders Ranges [SFR], Olary Ranges [OR]; Contact Zone (CZ); *C. decresii* (Mainland South [MS], and Kangaroo Island [KI]). Two outlying admixed individuals (from the 95% confidence ellipse) were those found in the geographic range of *C. decresii* (MS).

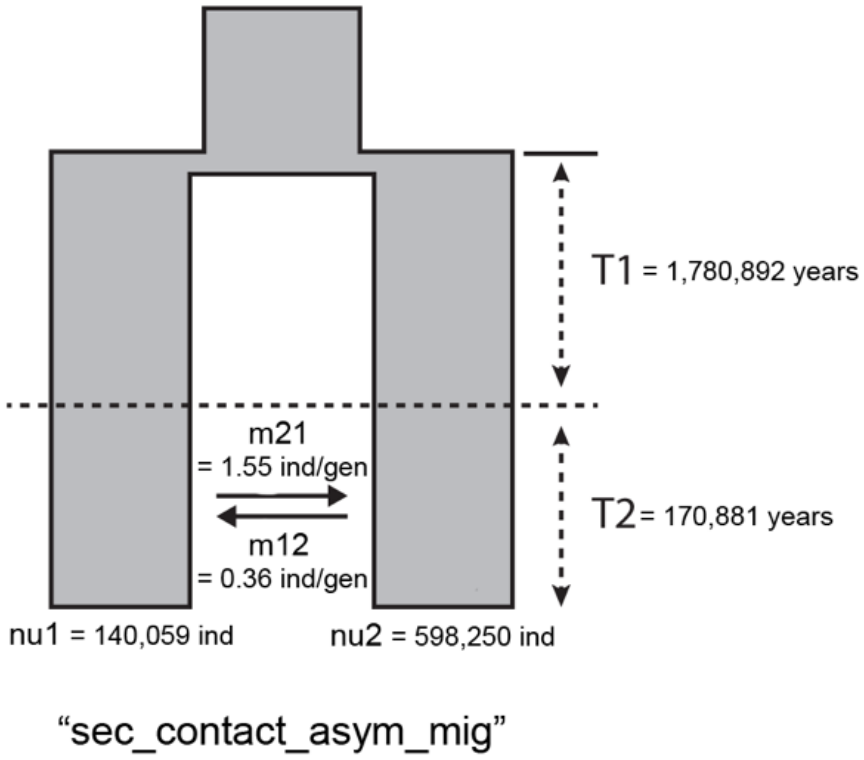

Figure 4. Schematic representation of the top demographic model from δaδi analysis. Populations 1 and 2 are *C. decresii* and *C. modestus* (pooled with admixed individuals) respectively. Converted values are provided for times (T1, T2, T3; in years), migration rates (m12, m21; in individuals per generation) and population sizes (nu1 and nu2; in number of individuals).

1002

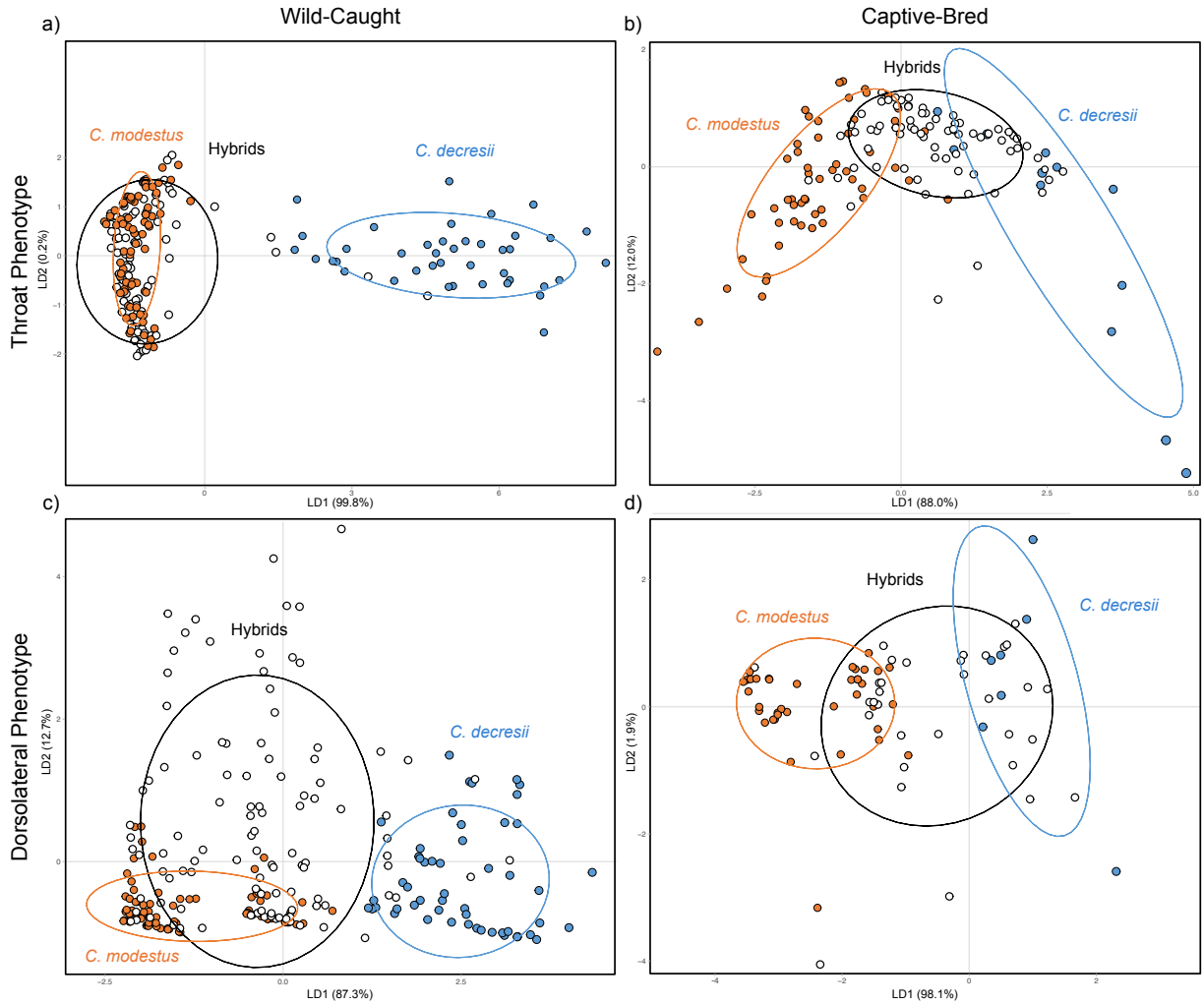

1003

1004

1005 **Figure 5**. Biplots of linear discriminant analyses on (a, b) throat and (c, d) dorsolateral
1006 phenotype variables for (a, c) wild-caught individuals along the contact zone transect and (b,
1007 d) captive-bred pure and F1 hybrid offspring. 95% confidence ellipses are shown.

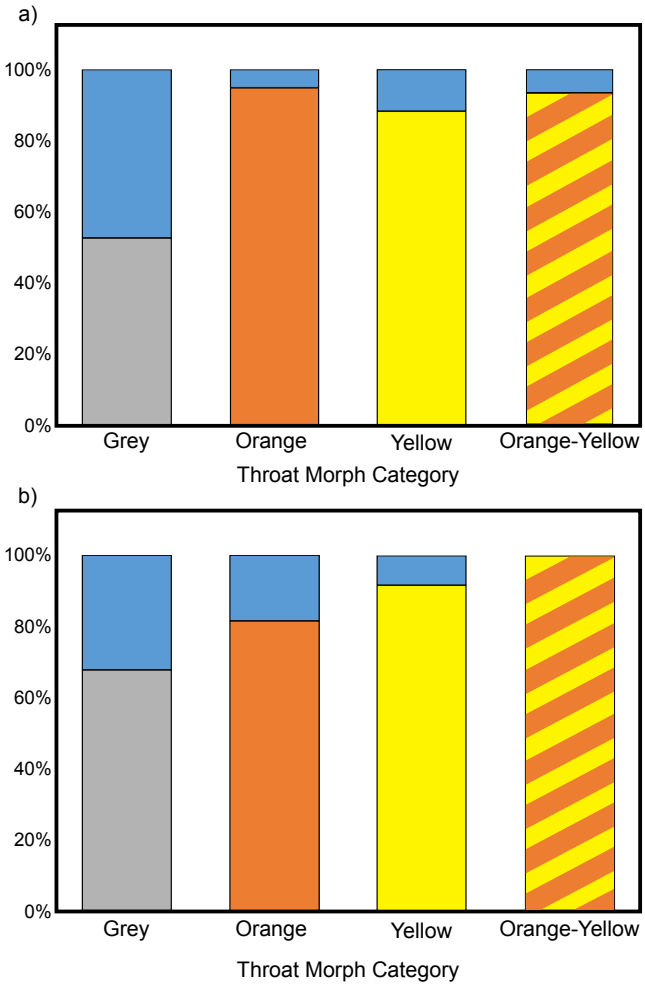

Figure 6. Percentage of individuals in each throat morph category which exhibit a degree of blue coloration on the throat for (a) wild-caught male hybrids (grey N = 19, orange N = 39, orange-yellow N = 15, yellow N = 17) and (b) captive-bred F1 hybrids (both sexes; grey N = 31, orange N = 27, orange-yellow N = 2, yellow N = 12).

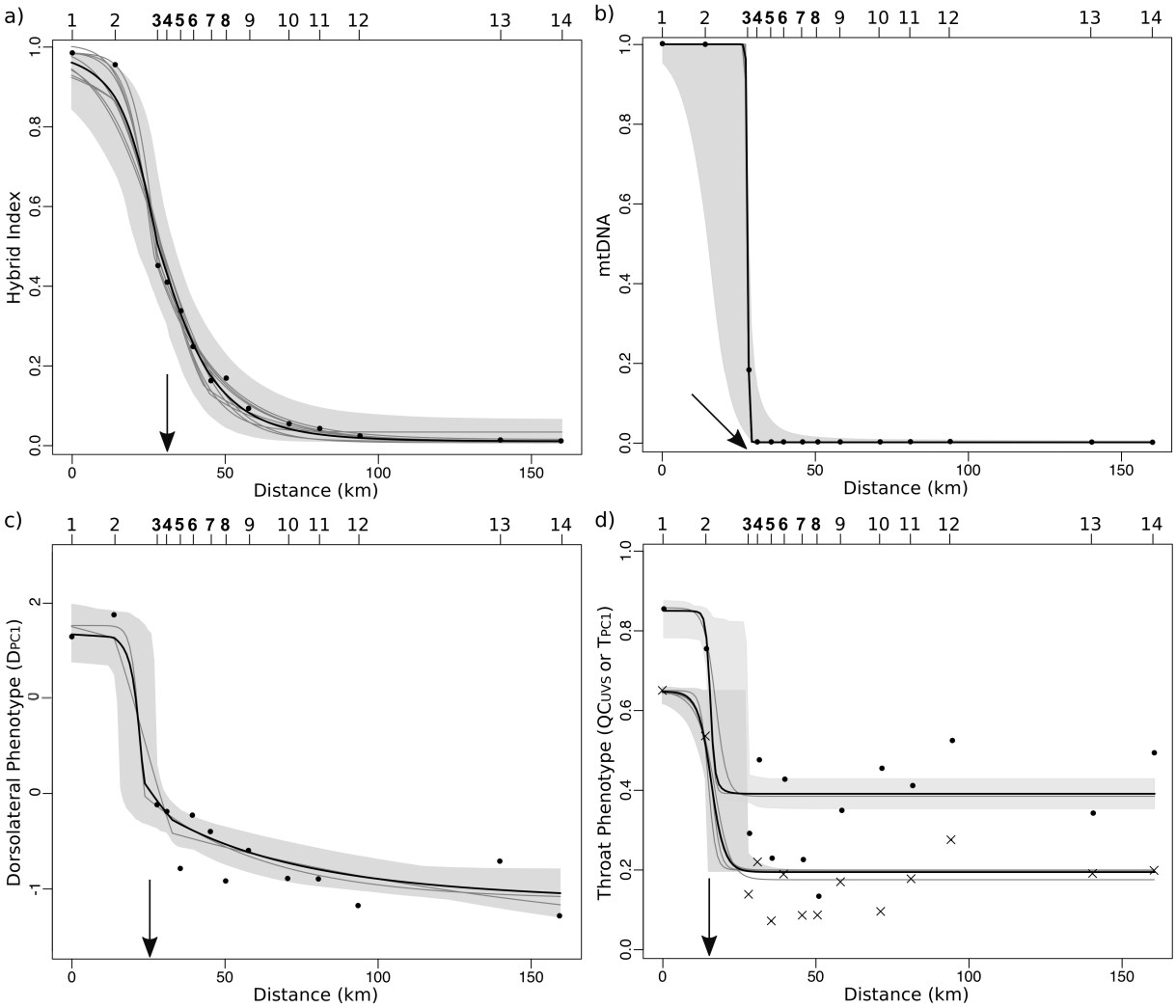

Figure 7. AICc model-averaged geographic clines (black) and credible regions, clines comprising the 95% confidence set of models (grey), and observed frequencies at each site for (a) the hybrid index estimated from 1333 loci (N = 154), (b) mtDNA haplotype frequencies (N = 74), (c) dorsolateral phenotype (D_{PC1}; N = 233), and (d) throat phenotype clines (N = 204 for both): quantum catch of UV receptor (QC_{UVS}; lower cline, frequencies shown with '×' symbols) and throat colouration (T_{PC1}; upper cline). Numbers along the top refer to sampling sites (see Table S2 for sample sizes at each site), bolded sites (3 – 8) comprise the contact zone. Transect distance is the cumulative distance from the southern-most population with increasing distance northwards. Arrows indicate cline centres; throat phenotype clines have essentially the same centres and are indicated with one arrow.